Boron Nitride Nanotube Impurity Detection and Purity Verification

Mahmoud S. Amin,¹ Tucker Ethan Molin,² Carlo Tampubolon,² David E. Kranbuehl,^{2,*} Hannes C. Schniepp¹

- 1) Department of Applied Science, The College of William & Mary
- 2) Department of Chemistry, The College of William & Mary
- *) dekran@wm.edu

ABSTRACT

Interest in boron nitride nanotube (BNNT) composites has grown exponentially because of BNNTs' unique properties. The vast majority of papers have used a BNNT material without identifying its purity. Impurities are known to misrepresent the BNNT concentration effect on performance properties and can have their own property effect on performance. A recent paper reported a major improvement in a biological application after purification. This demonstrates the need for a discussion of the optimum procedures to detect each impurity and quantify its degree of removal after a purification process. Here we evaluate the ability of thermal gravimetric analysis (TGA), Fourier transform infrared spectroscopy (FTIR), nuclear magnetic resonance (NMR), X-ray diffraction and non-resonant Raman to detect BNNT's boron, boron oxide and varying forms of boron nitride impurities. We discover that unstacked boron nitride impurities are present and detected in BNNT using non-resonant Raman. Stacked crystalline hexagonal boron nitride (h-BN) is separately detected using X-ray diffraction. We show that in contrast to aggressive high temperature purification methods that attack the boron nitride tubes, a low temperature hydrocarbon purification procedure removes both unstacked boron nitride impurities as well as stacked h-BN. We demonstrated the ability of non-resonant Raman spectra to detect and quantify the degree of removal of both forms of unstacked and stacked boron nitride impurities, of the ability of TGA to detect and quantitively verify the absence of boron and of FTIR techniques to detect and quantitavely verify degree of removal of boron oxide.

INTRODUCTION

Interest in boron nitride nanotube (BNNTs) has grown exponentially over the past two decades because of BNNTs' unique mechanical and thermal performance properties. 1-4 BNNT has exceptional strength, a Young's modulus near 1.3 TPa and is thermally stable in air up to 850 °C. BNNTs also have a high thermal conductivity greater than copper yet unlike most high thermal conductivity materials BNNT is an electrical insulator. 5 Thus, they are potentially an important material for thermal management in electronic devices. Until recently, researchers have used BNNT materials without identifying its purity. 6-11 Impurities are known to affect a material's performance properties. Impurities misrepresent the BNNT concentration effect on performance, and each impurity can have its own property effects on performance. Recently a 2020 paper reported purification of BNNT resulted in exceptional improvement in a biological application. This demonstrates the need for highly sensitive impurity detection measurement methods and measurement procedures that assess quantitatively the degree of impurity removal after a purification process.

The three impurities known to be produced during the synthesis of BNNTs, whether fabricated during low temperature synthesis methods (below 2000 °C) or by the high temperature pressure synthesis method (HTP) are boron, boron oxide, and the various forms of boron nitride impurities^{5,13}. These impurities hinder as a function of

their concentration the ability of BNNT's to enhance performance properties. Several research groups are aware of characterization techniques to assess the purity of BNNTs. ^{13–20} A few papers focus on procedures for the removal of impurities. ^{13–20} Most of these papers describe aggressive high temperature and/or strong chemical methods which damage the tubes and are unable to remove all of the impurities. These papers are significant contributions toward purification of BNNT. The most recent paper uses a high temperature innovative chemical procedure to remove impurities. ²⁰ It has a full discussion of impurity detection techniques including ¹¹B NMR and a range of spectroscopy and microscopy methods. Yet these high temperature and /or strong chemicals methods attack the tubes as well as the impurities. And after purification some boron impurities remain. Most important there is an absence of detection procedures which quantify the degree to which each of the three known impurities in BNNT have been removed.

This paper characterizes in detail the ability of five instrumental methods to detect the presence of each of the impurities in a BNNT material and to evaluate the degree of removal of each impurity after a purification process. Given the potential importance of BNNT in so many applications, detecting the impurity and the degree to which a purification process removes that impurity is essential for a valid interpretation of the enhancement of a desired property by that BNNT material. Here three different BNNT materials fabricated at different times over the past four years during the development of improved HTP procedures to optimize production and produce tubes of increasing purity are examined. Using five spectroscopic techniques, the ability of the technique to detect each impurity and verify its degree of its removal is discussed and evaluated. We demonstrate how TGA can detect boron impurities by comparing the weight changes as boron oxidizes at specific temperatures compared to pure BNNT. We discuss how the positions and line shape of an X-ray spectrum can be used to assess the presence of h-BN and determine the extent of its removal. We explore the ability of boron NMR to detect BNNT impurities. We examine the ability of FTIR to detect the presence and degree of removal of boron oxide and evaluate the ability of peak height and area to detect the presence of h-BN. For the first time, we demonstrate the ability of the nonresonant Raman spectra to detect the presence of both unstacked boron nitride impurities as well as stacked h-BN boron nitride and their degree of removal after a purification procedure. This paper uses these five techniques to assess impurity content of three BNNT materials after four degrees of purification; a) as-produced BNNT, BNNT that does not undergo any type of purification, and therefore contains a large percent of impurities, b) as-received BNNT, BNNT material that underwent a purification process for the removal of boron and boron oxide at BNNT LLC, c) BNNT oxidized and washed, as-produced BNNT that underwent purification in our William & Mary laboratory for removal of boron and boron oxide, and d) heptane purified BNNT, BNNT that underwent our recently reported heptane purification method for removal of h-BN impurities. 12 Each spectroscopic and thermal technique's ability to detect and quantify degree of an impurity's removal at each purification state is evaluated.

MATERIALS

As a known form of a boron nitride impurity, reagent grade h-BN was used and purchased from Sigma Aldrich. Reagent grade boron oxide and boron, the other two known impurities were also purchased from Sigma Aldrich.

Three different BNNT materials produced at BNNT LLC (Newport News, VA, US) using the high temperature and pressure (HTP) method are examined. They are labeled BNNT 1, BNNT 2, and BNNT 3. They were produced during the period 2015 to 2019 at BNNT LLC. The difference between the three batches are in the boron target heating technology and the chamber pressure conditions. This information under non discloser agreement and this is what we can reveal about the batches.

PURIFICATION PROCEDURES

The boron in as-received BNNT was oxidized in an oven in air at 550 °C for 3 hours. Then the BNNT containing the now oxidized boron, plus the existing boron oxide in the as-received BNNT, was inserted into a glass tube. The front half of the glass tube which contained the BNNT was heated to 120 °C to 130 °C. Steam was then continuously passed through the tube. The water which condensed at the tube end was collected periodically and dried to detect boron oxide. When boron oxide crystals were no longer present after evaporation of the water, the flow of steam was stopped. Then the steam washed BNNT to remove the oxidized boron and existing boron oxide impurities was removed.

Boron nitride impurities were removed using our previously described moderate temperature high yield hydrocarbon solvent processing method. It involves placing the BNNT in a high-pressure glass tube filled with heptane, heating at $90\,^{\circ}\text{C}$ for 3-5 hours to detach the boron nitride impurities from the BNNT.

CHARACTERIZATION METHODS

Thermal gravimetric analysis (TGA). TGA was used to detect and verify the absence of boron in the BNNT materials. By heating the BNNT samples at 550 °C in air using a TA Q500 instrument, the boron impurities were oxidized to boron oxide and the BNNT gained weight.

X-ray diffraction (XRD). XRD analysis was performed using a Bruker APEX DUO diffractometer equipped with an APEX II CCD Detector and a micro-focus copper K_{α} source (wavelength λ =1.54 Å). The samples were prepared by compressing 20 mg of BNNT material in discs with a diameter of 3 mm. To address possible inhomogeneity in the BNNT samples, different locations on the BNNT disc were measured.

Fourier transform infrared spectroscopy (FTIR). FTIR measurements were made using a Shimadzu IRTracer-100 FTIR spectrophotometer with a reflection ATR accessory on the as-received BNNT, the heptane-purified BNNT and the h-BN. An average of 32 runs with a resolution of 4 cm⁻¹ was used.

Raman spectroscopy. Raman data was collected using a Renishaw in Via dispersive Raman spectrometer using 514 nm with an excitation power of 40 mW and a $100 \times$ objective with a 0.90 NA. The samples for the as-received BNNT and purified BNNT were prepared by compressing the materials into 3 mm diameter discs for higher density and a better Raman signal. The Raman spectrum had a broad background over the range of $500-7000~\text{cm}^{-1}$ due to fluorescence. This background was removed using a second-order polynomial fit.

Nuclear magnetic resonance (NMR). MAS NMR experiments of the BNNT 11 B-containing impurity compounds were performed on a 750 MHz (11 B frequency of 240.73 MHz) wide bore (Bruker, Billerica, MA) spectrometer using a Bruker BL3.2 HX 3.2 mm MAS probe tuned to 1 H 11 B. Spinning was regulated at 8.0 kHz \pm 5 Hz using a Bruker MAS II pneumatic MAS controller. These experiments employed quadra polar echoes of 0.5 ms.

Thermal gravimetric analysis (TGA) was used to assess its ability to detect the impurities in BNNT. A temperature ramp at 10 °C/min in air up to 1000 °C on boron, boron oxide and h-BN (Sigma Aldrich materials) was conducted to identify the oxidation temperature of these three known impurities created during the HTP fabrication method. The TGA figures display the percentage weight change during a 10 °C/min ramp in air to 1000 °C.

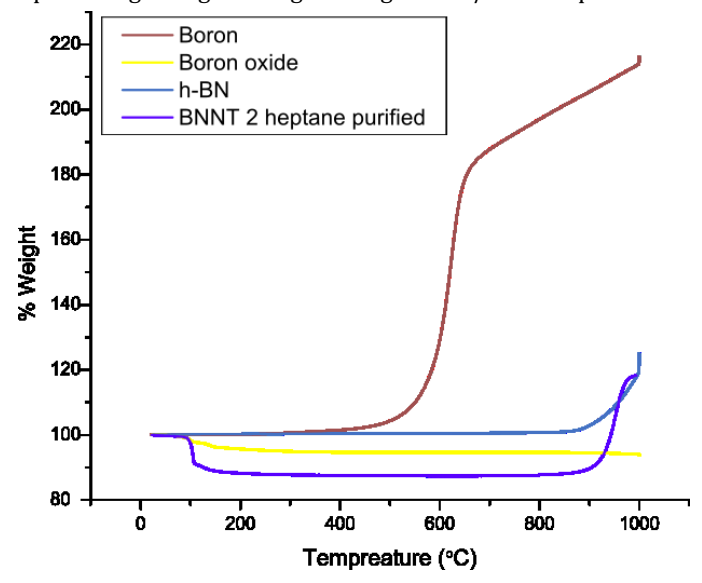


Figure 1: Thermal gravimetric analysis spectra of heptane purified BNNT and different impurities for a baseline comparison.

Figure 1 compares the percentage weight change of BNNT heptane purified (purple curve) with respect to boron (red curve), boron oxide (yellow curve) and h-BN (blue curve). The spectrum shows that boron experiences oxidation beginning around 300 °C and oxidizes more rapidly as 400 °C is approached. The rate of weight change then decreases as the temperature approaches 600 °C. Boron oxide is shown to be stable over the entire temperature range. The h-BN begins to oxidize around 825–850 °C. The BNNT 2 heptane was stable up to a slightly higher temperature near 850–900 °C but then oxidizes more rapidly than h-BN. Although the boron appeared to oxidize at around 300 °C in Figure 1, other experiments have shown that BNNT's boron impurities oxidize around

200 °C. This might be explained by the nanoscale particle size nature of the boron impurities²¹ formed during the HTP synthesis method which are expected to be more reactive than Aldrich h-BN material.

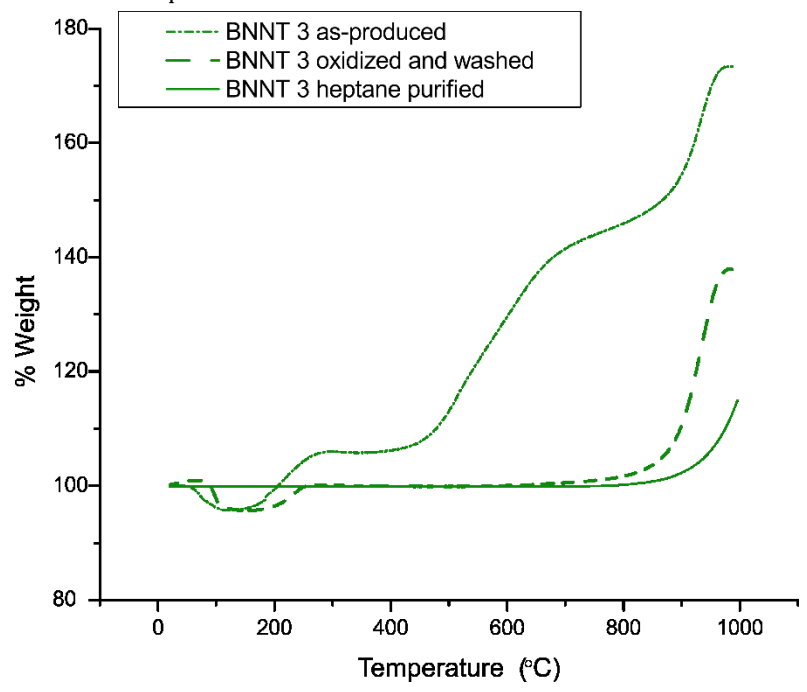


Figure 2:TGA spectra of BNNT 3 samples at different purification stages.

Figure 2 displays the percentage weight change for the most recently fabricated as-produced BNNT 3 material. Also displayed are BNNT 3 after oxidation at 550 °C for three hours in air to oxidize boron and then washed to remove all boron oxide; and BNNT 3 after having had boron nitride impurity removed by treatment with heptane under pressure at 90 °C for 3–5 hours. Both the BNNT 3 as-produced and boron-boron oxide purified samples show that BNNT is highly hydroscopic picking up several percent water. The heptane purified BNNT shows no water loss as it had been previously run on the TGA to make certain the heptane was completely removed. As shown in Figure 2, there is an increase in the percentage weight gain at 200 °C and again as the temperature approached 400 °C. Based on Figure 1, these weight gain results demonstrate that boron exists in as-produced BNNT.

Figure 1 and Figure 2 indicate the boron impurity undergoes a complex oxidation process. As has been previously reported in a study of the kinetics of boron oxidation.²² the boron particles become coated with an oxide layer, which decreases the rate of oxidation up to temperatures approaching the temperature where h-BN and BNNT also decompose. Figure 2 showed that oxidized and washed BNNT 3 material, aside from moisture removal, shows no weight change until temperatures where both h-BN and BNNT begin to oxidize. Similarly, the heptane purified BNNT 3 material showed no weight loss until the purified boron nitride tubes begin to decompose.

Figure 1 and Figure 2 clearly demonstrates that a TGA analysis of percentage weight gain can be used to detect the presence of boron and that the absence of a change in weight during a temperature ramp indicates its removal. To quantify the degree of removal when a TGA ramp shows no detectable change in weight, we assume a 10mg sample and a detection noise limit of 0.01mg, an instrument sensitivity of .001mg, along with the fact that the weight will continue to rise due to oxidation as in Figures 1 and 2. Thus no detectable change in weight verifies that 99.9% of the boron was removed during purification and the boron content in the sample is less than 0.01 mg.

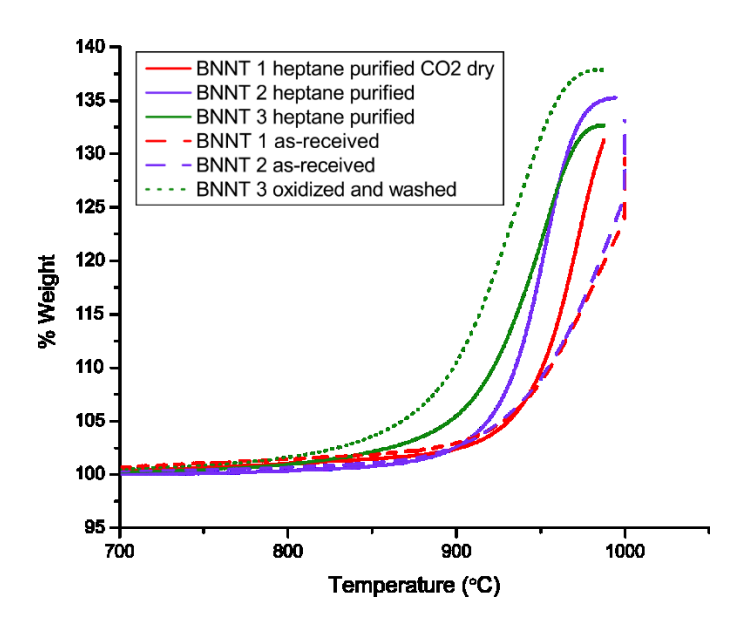


Figure 3: TGA spectra zoom in from 700 °C-1000 °C to show the difference in the starting oxidation temperatures between different BNNT materials.

Figure 3 focuses on the high temperature stability of the three different batches of BNNT 1, 2 and 3 produced over four years after boron and boron oxide removal compared to these three materials after heptane purification to remove boron nitride impurities. The results showed both BNNT 1 and BNNT 2 materials are stable up to 900°C. BNNT 3 oxidized and washed started to decompose near 800 °C. BNNT 3 heptane purified started to decompose near 850 °C. Boron nitride impurity defects would oxidize more easily which could account for weight change at a lower temperature and provide evidence that purification removed these impurities. Similarly, differences between BNNT 1, 2 and 3 in their tubes' crystalline structure and the number of crystal defects which act as weak sites could explain the onset of oxidation at slightly different temperatures.

The similar onset of weight change in two BNNT 1 and two BNNT 2 materials before and after heptane purification in Figure 3 suggests that in these materials their boron nitride impurities and BNNT oxidize at the same temperature. These BNNT results indicates that high temperature removal of boron nitride impurities can also destroy the boron nitride tubes In summary, Figures 1–3 demonstrate that a TGA ramp detects the presence of boron in BNNT and that the absence of weight change demonstrates the purification process has removed 99.9% of the boron.

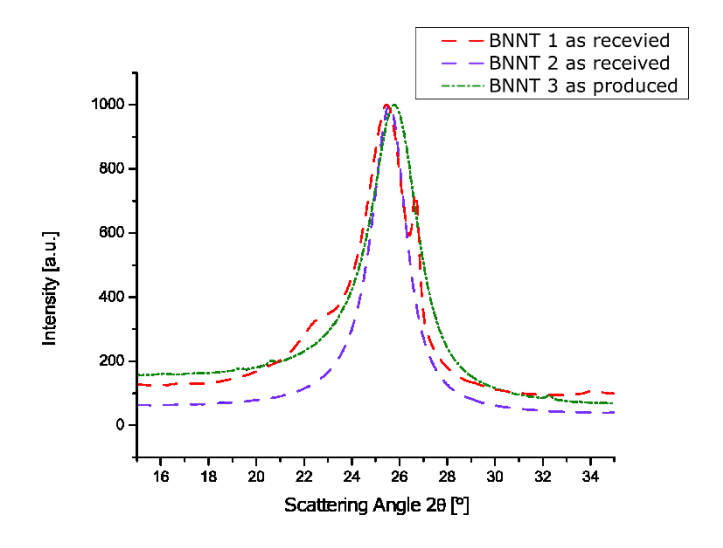


Figure 4A: X-ray diffraction of BNNT 1, BNNT 2, and BNNT 3 before heptane purification

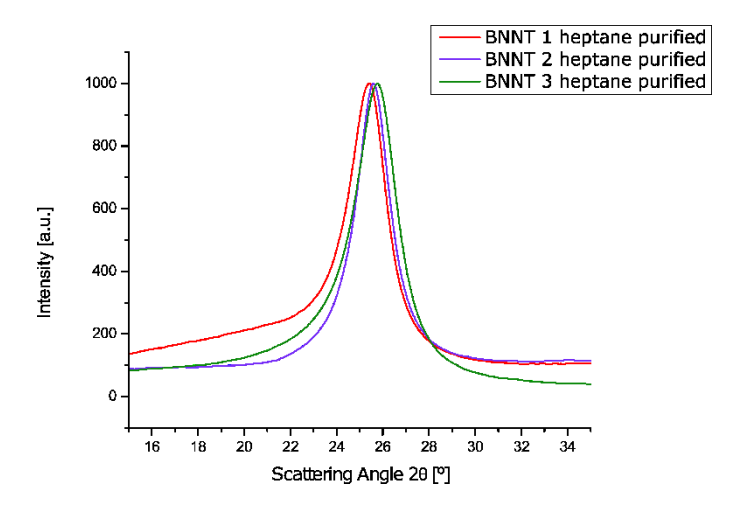


Figure 4B: X-ray diffraction of BNNT 1, BNNT 2, and BNNT 3 after heptane purification

The X-ray Diffraction spectra before and after heptane purification are shown in Figure 4A and 4B respectively. In an earlier report on development of the heptane purification method, the X-ray diffraction peak in BNNT 1 at 26.69° with a shoulder peak at 26.69° was shown to detect stacked crystalline h-BN.5 What is different from BNNT 1 is that BNNT materials 2 and 3 do not display BNNT 1's h-BN shoulder peak at 26.69°. This indicates BNNT 2 and BNNT 3 do not contain h-BN. After heptane purification of BNNT 1 where it was shown 99% of the h-BN was removed¹², only a BNNT peak at 25.42° was observed.²³ The BNNT 1 X-ray peak values in Table 1 can be compared with the as-received peaks of BNNT 2 at 25.58°, BNNT 3 at 25.76°, and their heptane purified peaks at 25.60° and 25.76°, respectively. Each batch of BNNT made at various times will have its own characteristic tube diameters resulting from the multi walled structures created by the HTP fabrication conditions. As a result, each BNNT material will have slightly different X-ray diffraction peak positions and full width half maximum (FWHM) values reflecting that HTP process's creation of the tube structure and crystal heterogeneity. The FWHM values of BNNT 2 and BNNT 3 change very little to not at all after heptane purification in contrast to the BNNT 1 material with h-BN. The significant change in BNNT 1's FWHM value after h-BN's removal is expected as the h-BN shoulder peak overlaps the BNNT peak. This makes the as-received BNNT 1 peak's shape broader and asymmetric as it contains h-BN. This is in contrast with both BNNT 2 and BNNT 3 before heptane purification where the BNNT peak's shape is symmetric. This further supports the observation that there is a little to no h-BN in BNNT 2 and in BNNT 3. In

summary, X-ray spectra can detect stacked h-BN boron nitride impurities and as previously discussed the absence of that shoulder peak after purification indicates 99% of the h-BN was removed.

Table 1: X-ray diffraction peak positions and full width half maximum of different BNNT materials

Sample ID	Peak	Peak position [°]	FWHM [°]
As-received BNNT 1	h-BN	26.66	0.80
	Main	25.40	2.42
Heptane purification BNNT 1	Main	25.33	1.96
BNNT 2	Main	25.58	1.85
BNNT 2 heptane	Main	25.60	1.95
BNNT 3	Main	25.78	2.67
BNNT 3 heptane	Main	25.76	2.36

Raman spectroscopy has been used for the characterization of BNNTs in the literature for many years. A thorough study has shown that BNNTs show a peak at $\approx 1,370~\rm cm^{-1}$ when studied using resonant Raman spectroscopy, carried out at $\lambda = 229~\rm nm.^{25}$ In non-resonant Raman spectroscopy, BNNTs did not show any characteristic peaks in this spectral region. In contrast, h-BN in non-resonant Raman spectroscopy does show a pronounced peak at 1364.6 cm⁻¹.5.25 Consequently, non-resonant Raman spectroscopy is a powerful technique to detect the presence of h-BN in BNNT. In our experiments, we used non-resonant Raman spectroscopy with an excitation wavelength of $\lambda = 514~\rm nm.$

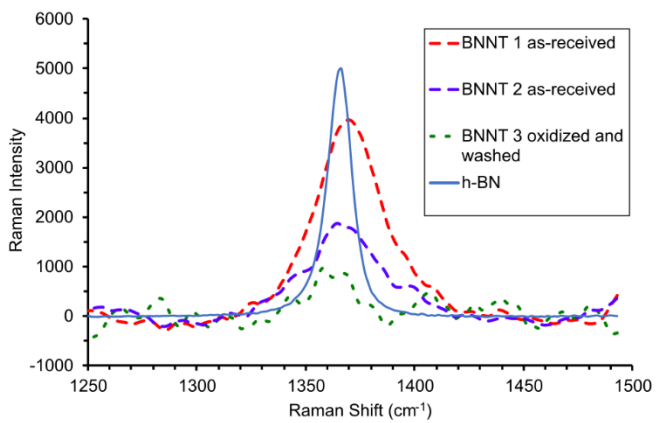


Figure 5: Non-resonant Raman spectra of as-received BNNTs overlaid with h-BN. The as-received BNNTs showed much broader Raman peaks near the h-BN Raman peak at 1365 cm⁻¹

Figure 5 shows the non-resonant Raman spectral spectrum for each of the three BNNT materials before heptane purification along with the Raman spectrum for h-BN. All three BNNT materials show slightly different peak positions and a broader peak shape relative to h-BN. As shown and previously discussed these spectra are similar to the location of the Raman peak observed for h-BN. 12,25 What is surprising here is that BNNT 2 and BNNT 3 have a non-resonant Raman peak similar to BNNT 1 in spite of the fact that these two BNNT materials do not have h-BN as demonstrated by absence of a h-BN shoulder peak in their X ray spectra.

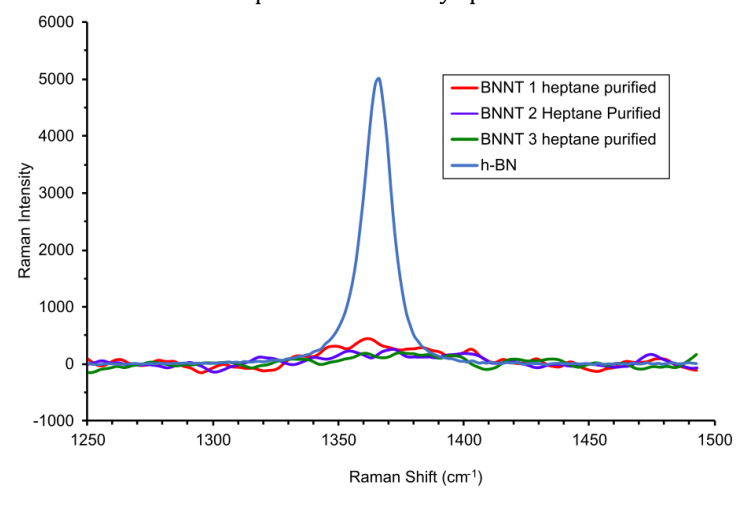


Figure 6: Non-resonant Raman spectra of BNNT heptane purified overlaid with h-BN.

Figure 6 shows an overlay of the spectral shift of the three BNNT materials after heptane purification. The peak is absent indicating there is no h-BN, but as the X-ray results show there was no detectable h-BN in these two BNNT materials resulting from the HTP fabrication process at that time. Hence, the non-resonant Raman peak in BNNT 2 and BNNT 3 is detecting boron nitride impurities which we characterize as unstacked in contrast to the stacked crystalline h-BN. Particularly important is the absence of this peak in heptane purified BNNT 2 and BNNT 3. This verifies removal of these unstacked boron nitride impurities using the heptane purification procedure. Further

based on the BNNT 2 and BNNT 3 unstacked boron nitride impurity spectra, the broad shape of the as-received BNNT 1 Raman peak in Figure 5 indicates that BNNT 1 contains unstacked boron nitride impurities in addition to crystalline h-BN.

To establish the degree of removal of the boron nitride impurities when the peak is absent, the non-resonant Raman peak for each BNNT material in Figure 5 was fit to a Lorentzian and then subtracted from the Raman spectra to obtain the noise level. Using the ratio of the peak height to the noise level detection limit shows the degree of removal ranges from 98% in BNNT 1, 95% in BNNT 3, to 80% in BNNT 2. See Supporting Information, degree of removal of boron nitride impurities.

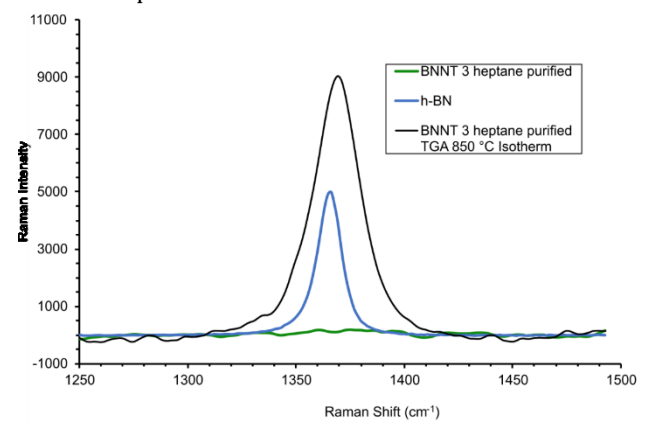


Figure 7: Non-resonant Raman spectrum for BNNT 3 heptane purified before and after TGA 850° isotherm and the h-BN Raman peak.

Figure 7 displays the Raman spectrum for a sample of BNNT 3 after it was heated at 850 °C for 180 minutes. The results show that the creation of this peak at $\approx 1,370~\rm cm^{-1}$ after heating at 850 °C strongly indicates the tubes decomposed to boron nitride impurities. The similarity of the shape of the peak to h-BN peak suggests primarily stacked h-BN boron nitride impurities were formed. A major impurity created during high temperature oxidation of BNNT is boron oxide. As such, we verified that boron oxide does not have a non-resonant Raman peak in the range of Figure 7. This result further supports use of non-resonant Raman to detect both stacked boron nitride impurities and unstacked non boron nitride impurities. It also supports earlier TGA results indicating high temperature methods to remove boron nitride impurities are destroying BNNT tubes and adding to the amount of h-BN boron nitride impurities.¹³

In summary, for the first-time unstacked boron nitride impurities have been identified in BNNT. It has been shown that non-resonance Raman spectroscopy is able to detect the presence of stacked crystalline h-BN and to detect unstacked boron nitride impurities. Equally important, between the X-ray and Raman spectra, the type of boron nitride impurity present is identified. Most important, the absence of the Raman peak indicates removal of not only stacked crystalline h-BN as previously shown⁵ but also unstacked h-BN impurities and that non resonant Raman is able to quantitatively verify boron nitride removal due to a purification.

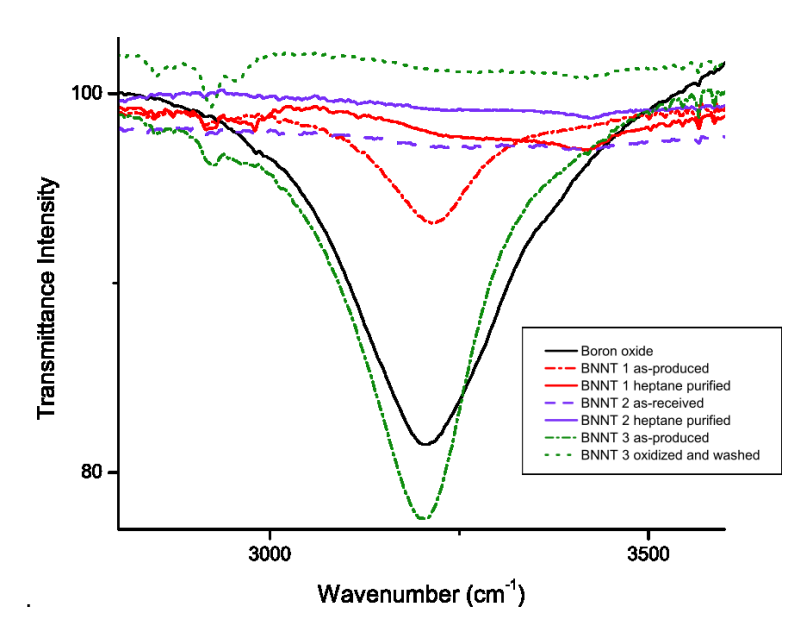


Figure 8: FTIR spectra zoom in from 2800-3600 cm-1 of BNNT materials at different purification stages

Fourier transform Infrared spectroscopy (FTIR), like TGA, X-ray, NMR and non-resonant Raman spectroscopy, was used as an analytical tool to detect two of BNNT's impurities, boron oxide and h-BN. Figures 8 and 9 are an expansion of the FTIR spectra. Figure 8 displays the high frequency side and Figure 9 displays the low frequency portion of the FTIR spectra, first we focus on detecting boron oxide. Figures 8 and 9 display boron oxide's three clearly identifiable peaks at 3203 cm⁻¹, 1355 cm⁻¹, and 696 cm⁻¹. The last two peaks are obscured underneath the two strong peaks for h-BN and BNNT at 1317 cm⁻¹ and 783 cm⁻¹ in Figure 9. Figure 8 focuses on the isolated boron oxide peak at 3203 cm⁻¹ This peak's height reflects the variation in the amount of boron oxide after differing levels of purification. To address the amount of boron oxide, the spectra were normalized to make the 1317 cm⁻¹ peak heights equal. Figure 8 shows that the as-produced BNNT 3 did contain a significant amount of boron oxide and that it was removed during the boron oxidation and steam wash purification process at William & Mary. Figure 8 also shows the presence of boron oxide in as-produced BNNT 1 as well as its removal in heptane purified BNNT 1. And Figure 8 based on the normalized FTIR spectra, shows the presence of a much smaller amount of boron oxide in as-received BNNT 2 and its removal in heptane purified BNNT 2. These results demonstrate the use of FTIR to detect the presence of boron oxide and to verify the removal of boron oxide impurities. They also suggest that removal of residual boron oxide impurities occurs during heptane purification.

To establish degree of removal of the boron oxide impurities when the FTIR 3203 cm⁻¹ peak is absent, the FTIR peak for as-produced BNNT 1 and BNNT 3 was fit to a Lorentzian and then subtracted from the FTIR 3203 cm⁻¹ spectrum to obtain the noise level. Using the ratio of the peak height to the noise level as a measure of the detection limit leads to a degree of boron oxide removal of 98% in BNNT 1 and 99% in BNNT 3. See Supporting Information, degree of removal of boron oxide.

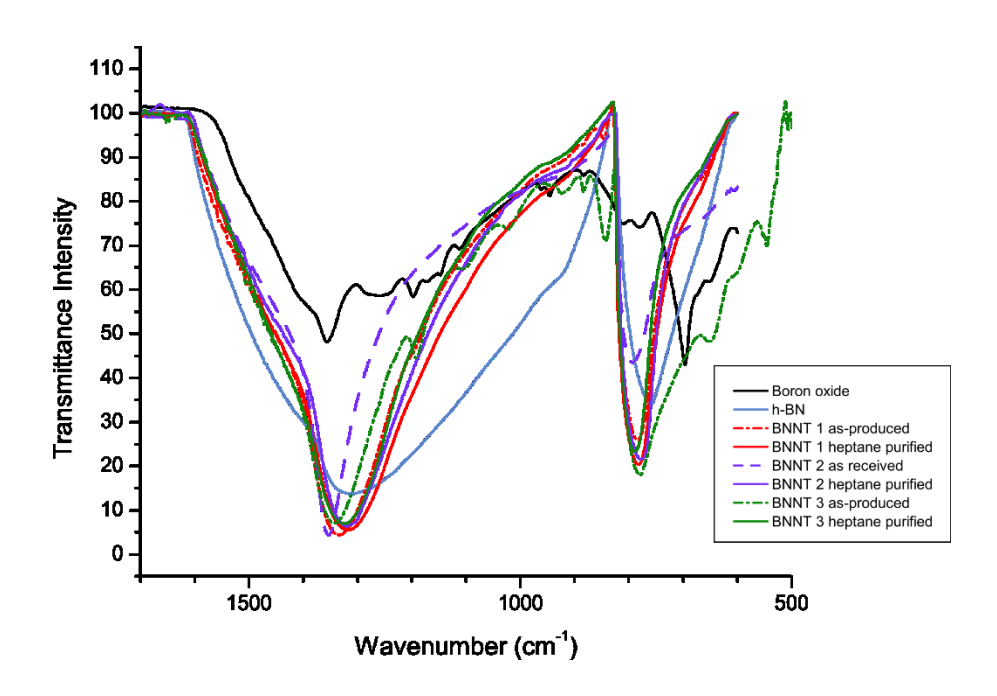


Figure 9 FTIR spectra zoom in from 500–1700 cm⁻¹ of different BNNT materials at different purification stages

The spectra were normalized to create identical peak heights at 1317 cm⁻¹.

Figure 9 focuses on h-BN's and BNNT's two peaks before and after heptane purification. These two peaks are attributed to out of plane buckling near 1317 cm⁻¹ and in-plane optical phonon modes near 783 cm⁻¹. The expansion of this region displays the effect of an appreciable concentration of boron oxide on the BNNT peaks in the asproduced BNNT 3. The large change in shape of the BNNT 783 cm⁻¹ peak reinforces the effect of the high concentration of boron oxide in as-produced BNNT 3 relative to as-produced BNNT 1 and in as received BNNT 2. A narrowing of the width of these FTIR peaks in purified BNNT 3 versus as-produced BNNT 3 and to a lesser extent for BNNT 1 and BNNT 2 after heptane purification are an indication of boron nitride impurity removal during heptane purification.

Previous work has proposed and explored a peak height ratio method utilizing the FTIR spectra of these h-BN and BNNT peaks to detect the presence of h-BN impurities in a BNNT material and to quantify h-BN's concentration. ^{5,26} This earlier work proposed that the ratio of the 783 cm⁻¹ to 1317 cm⁻¹ peak in h-BN was close to 1 and that h-BN removal from BNNT samples would result in a decrease in this ratio. It was also proposed that such a decrease could be used to quantify h-BN removal. This idea was explored here on BNNT 1 which contains h-BN and on BNNT 2 and BNNT 3 which contain unstacked boron nitride impurities. No correlation was found between the degree of h-BN removal or unstacked boron nitride impurities and a decrease in the ratio of the 783 cm⁻¹ peak height to the 1317 cm⁻¹ peak height. This is in agreement with another recent publication. ²⁰ Using a peak area ratio method however showed a decrease in the ratio with purification. See Supporting Information, peak area ratio method.

It is well documented through theoretical predictions of the FTIR peak positions of these two modes of vibration that they vary depending on the tube diameter and the number of concentric tubes in the multiple walled tube sample. This is caused by these two variations in tube structure affecting the inter and the intra-tube boron nitride bond strengths.²⁷ These predictions imply that the FTIR spectra of samples will differ as the number of concentric tubes and tube diameters vary in a BNNT material. Most BNNT samples contain a mix of different tube diameters and multi walled tubes. Thus, these two peaks in the FTIR spectra for most BNNT samples will be wider reflecting the varying covalent boron nitride bond strengths due to the differing tube structures. This fact is supported by the literature concerning the FTIR spectrum of a multi-walled BNNT material, where the 1300 cm-1 peak is a bimodal combination of two broad absorption peaks.²⁶ Thus, we believe this method of quantifying h-BN concentration through a change in peak height ratios only works well in a BNNT sample of single-walled, uniform diameter tubes. Hence most as-produced BNNT material has its unique FTIR spectra that reflects the varying bond strengths in the BNNT material resulting from that BNNT material's tube structure created during the HTP synthesis process. This

makes FTIR quantitative determination of h-BN impurity presence and removal very complex and not universal in application as it is tied to that particular BNNT's structure.

Clearly, FTIR is able to detect boron oxide, determine the relative amount of boron oxide present from the normalized FTIR spectra, and verify up to 97% of the boron oxide was removed during purification. Use of changes in the ratio of the areas of BNNT's two major FTIR peaks provides insight into changes in boron nitride impurity content but is dependent on that BNNT material's tube structure.

DISCUSSION

In an examination of three different BNNT materials fabricated over four years, four spectroscopy and a thermal technique are shown to successfully detect the presence and the removal, of the major impurities in as-produced BNNT, boron, boron oxide and boron nitride. The most powerful technique for detecting and quantitatively verifying boron nitride impurity removal after purification was non resonant Raman spectroscopy. For the first time the unstacked forms of boron nitride impurities in BNNT were detected as well as crystalline h-BN. For the first time removal of these unstacked boron impurities using low temperature heptane processing has been demonstrated. Particularly important, non-resonant Raman spectra in the range of 1361 cm⁻¹ is shown to display a peak when either or both h-BN and non-crystalline boron nitride impurities are present. The peak disappears when both h-BN and unstacked boron nitride impurities have been removed. The peak height to noise level was used to verify over 90% of the boron nitride impurities have been removed during a heptane purification process. Here non resonant Raman spectroscopy was shown to be a unique, powerful technique for assessing the presence of both unstacked and stacked h-BN impurities in BNNT and to quantitatively verify their removal.

We also explored the ability of boron NMR to detect impurities in BNNT. We found as previously shown that ¹¹B solid-state NMR with magic angle spinning (MAS) is able to detect the presence of boron, boron oxide, and h-BN.²⁰ In particular, the NMR spectra of h-BN are similar to BNNT. Thus, as it is the case for FTIR, this impairs the ability to assess the relative content of h-BN and BNNT in our samples. As a result, we did not pursue further the use of this method to quantify impurity removal.

CONCLUSIONS

It was demonstrated that TGA data during a temperature ramp detects boron impurity by a distinct weight gain as the temperature increases beyond 200 °C. A pure BNNT sample shows no change in weight up to 850–900 °C. Based on the .001mg sensitivity of the TGA instrument, a noise level below .01 mg, a TGA temperature ramp can verify 99.9% of the boron was removed during an oxidation and steam purification process. The BNNT's FTIR spectrum has a sharp peak at 3203 cm⁻¹ when boron oxide is present, a second peak at 696 cm⁻¹ and a broadening of the BNNT peaks due to boron oxide's third peak at 1355 cm⁻¹. The absence of these peaks indicates that boron oxide is absent. The height of boron oxides 3203 cm⁻¹ FTIR peak relative to the noise level can be used to verify up to 99% of the boron oxide was removed during steam purification. The presence of stacked h-BN boron nitride impurities is detected by a peak in the x ray spectra at 26.69°. and the absence of that peak after heptane purification verifies 99% of the h-BN was removed.

ASSOCIATED CONTENT

Supporting Information. "This material is available free of charge via the Internet at http://pubs.acs.org."

Ouantification of the sensitivity and detection limit of the Raman technique.

Quantification of the sensitivity and detection limit of the FTIR technique.

 $Quantification \ of the \ ability \ of the \ FTIR \ peak \ height \ and \ peak \ area \ ratio \ to \ correlate \ with \ boron \ nitride \ impurity \ content.$

AUTHOR INFORMATION-

Author Contributions

MSA and DEK designed the experiments and wrote the manuscript. DEK supervised the experiments. MSA carried out the experiments, with help from CT and EM. NMR experiments were conducted by AIG and supervised by MC. HCS led the project and supervised the data analysis and interpretation.

Notes

The authors declare no competing financial interest.12

ACKNOWLEDGMENT:

HCS and DEK acknowledge support from the Center of Innovative Technology under CRCF award MF17-032-AM and from the Office of Naval Research under Award N00014-18-1-2264. The authors acknowledge BNNT LLC for the BNNT materials. This material is based upon work supported by the National Science Foundation under Grant Nos. DMREF-1534428 and 1905902. The authors thank Dr. Alex Greenwood (William and Mary) and Dr. Riqiang Fu (National High

Magnetic Field Laboratory) for exploring the possibility of using 11B MAS NMR to quantify impurities in our BNNT samples.

ABBREVIATIONS

h-BN, hexagonal boron nitride; BNNT, boron nitride nanotube; TPH, high temperature pressure method for BNNT synthesis; XRD, X-ray diffraction; FWHM, full width half maximum; TGA, Thermal gravimetric analysis; FTIR, Fourier transform infrared; NMR, Nuclear magnetic resonance.

References

- (1) Lee, C.; Bhandari, S.; Tiwari, B.; Yapici, N.; Zhang, D.; Yap, Y. Boron Nitride Nanotubes: Recent Advances in Their Synthesis, Functionalization, and Applications. *Molecules* **2016**, *21* (7), 922. https://doi.org/10.3390/molecules21070922.
- (2) Chopra, N. G.; Luyken, R. J.; Cherrey, K.; Crespi, V. H.; Cohen, M. L.; Louie, S. G.; Zettl, a. Boron Nitride Nanotubes. *Science (New York, N.Y.)* **1995**, *269* (August), 966–967. https://doi.org/10.1126/science.269.5226.966.
- (3) Golberg, D.; Bando, Y.; Huang, Y.; Terao, T.; Mitome, M.; Tang, C.; Zhi, C. Boron Nitride Nanotubes and Nanosheets. *ACS Nano* **2010**, *4* (6), 2979–2993. https://doi.org/10.1021/nn1006495.
- (4) Verma, V.; Jindal, V. K.; Dharamvir, K. Elastic Moduli of a Boron Nitride Nanotube. *Nanotechnology* **2007**, *18* (43), 435711. https://doi.org/10.1088/0957-4484/18/435711.
- (5) Amin, M. S.; Atwater, B.; Pike, R. D.; Williamson, K. E.; Kranbuehl, D. E.; Schniepp, H. C. High-Purity Boron Nitride Nanotubes via High-Yield Hydrocarbon Solvent Processing. *Chem. Mater.* **2019**, *31* (20), 8351–8357. https://doi.org/10.1021/acs.chemmater.9b01713.
- (6) Yamaguchi, M.; Pakdel, A.; Zhi, C.; Bando, Y.; Tang, D.-M.; Faerstein, K.; Shtansky, D.; Golberg, D. Utilization of Multiwalled Boron Nitride Nanotubes for the Reinforcement of Lightweight Aluminum Ribbons. *Nanoscale research letters* **2013**, *8* (1), 1–6.
- (7) Belkerk, B. E.; Achour, A.; Zhang, D.; Sahli, S.; Djouadi, M.-A.; Yap, Y. K. Thermal Conductivity of Vertically Aligned Boron Nitride Nanotubes. *Applied Physics Express* **2016**, 9 (7), 075002. https://doi.org/10.7567/apex.9.075002.
- (8) Meng, W.; Huang, Y.; Fu, Y.; Wang, Z.; Zhi, C. Polymer Composites of Boron Nitride Nanotubes and Nanosheets. *J. Mater. Chem. C* **2014**, *2* (47), 10049–10061. https://doi.org/10.1039/c4tc01998a.
- (9) Bhuiyan, M. M. H.; Li, L. H.; Wang, J.; Hodgson, P.; Chen, Y. Interfacial Reactions between Titanium and Boron Nitride Nanotubes. *Scripta Materialia* **2017**, *127*, 108–112.
- (10) Quiles-Díaz, S.; Martínez-Rubí, Y.; Guan, J.; Kim, K. S.; Couillard, M.; Salavagione, H. J.; Gómez-Fatou, M. A.; Simard, B. Enhanced Thermal Conductivity in Polymer Nanocomposites via Covalent Functionalization of Boron Nitride Nanotubes with Short Polyethylene Chains for Heat-Transfer Applications. *ACS Applied Nano Materials* **2018**, *2* (1), 440–451. https://doi.org/10.1021/acsanm.8b01992.
- (11) Zhi, C.; Bando, Y.; Tang, C.; Honda, S.; Kuwahara, H.; Golberg, D. Boron Nitride Nanotubes/Polystyrene Composites. *Journal of Materials Research* **2006**, *21* (11), 2794–2800. https://doi.org/10.1557/jmr.2006.0340.
- (12) Lee, S.-H.; Kim, M. J.; Ahn, S.; Koh, B. Purification of Boron Nitride Nanotubes Enhances Biological Application Properties. *IJMS* **2020**, *21* (4), 1529. https://doi.org/10.3390/ijms21041529.
- (13) Marincel, D. M.; Adnan, M.; Ma, J.; Bengio, E. A.; Trafford, M. A.; Kleinerman, O.; Kosynkin, D. V.; Chu, S.-H.; Park, C.; Hocker, S. J. A.; Fay, C. C.; Arepalli, S.; Martí, A. A.; Talmon, Y.; Pasquali, M. Scalable Purification of Boron Nitride Nanotubes via Wet Thermal Etching. *Chemistry of Materials* **2019**, *31* (5), 1520–1527. https://doi.org/10.1021/acs.chemmater.8b03785.
- (14) Cohen, M. L.; Zettl, A. The Physics of Boron Nitride Nanotubes. *Physics Today* **2010**, *63* (11), 34–38. https://doi.org/10.1063/1.3518210.
- (15) Tiano, A. L.; Park, C.; Lee, J. W.; Luong, H. H.; Gibbons, L. J.; Chu, S.-H.; Applin, S.; Gnoffo, P.; Lowther, S.; Kim, H. J.; Danehy, P. M.; Inman, J. A.; Jones, S. B.; Kang, J. H.; Sauti, G.; Thibeault, S. A.; Yamakov, V.; Wise, K. E.; Su, J.; Fay, C. C. Boron Nitride Nanotube: Synthesis and Applications. In *Nanosensors, Biosensors, and Info-Tech Sensors and Systems 2014*; Varadan, V. K., Ed.; SPIE, San Diego, California, United States, 2014. https://doi.org/10.1117/12.2045396.
- (16) Maguer, A.; Arenal, R.; Jaffrennou, P.; Cochon, J. L.; Bresson, L.; Doris, E.; Mioskowski, C.; Loiseau, A. Purification of Single-Walled Boron Nitride Nanotubes and Boron Nitride Cages. *Journal of Nanoscience and Nanotechnology* 2007, 7 (10), 3528–3532. https://doi.org/10.1166/jnn.2007.829.
- (17) Koi, N.; Oku, T.; Inoue, M.; Suganuma, K. Structures and Purification of Boron Nitride Nanotubes Synthesized from Boron-Based Powders with Iron Particles. *Journal of Materials Science* **2007**, *43* (8), 2955–2961. https://doi.org/10.1007/s10853-007-1750-3.
- (18) Choi, J.-H.; Kim, J.; Seo, D.; Seo, Y.-S. Purification of Boron Nitride Nanotubes via Polymer Wrapping. *Materials Research Bulletin* **2013**, *48* (3), 1197–1203. https://doi.org/=.
- (19) Loiseau, A.; Willaime, F.; Demoncy, N.; Hug, G.; Pascard, H. Boron Nitride Nanotubes with Reduced Numbers of Layers Synthesized by Arc Discharge. *Physical Review Letters* **1996**, *76* (25), 4737–4740. https://doi.org/10.1103/physrevlett.76.4737.
- (20) Cho, H.; Walker, S.; Plunkett, M.; Ruth, D.; Iannitto, R.; Rubi, Y. M.; Kim, K. S.; Homenick, C. M.; Brinkmann, A.; Couillard, M.; Dénommée, S.; Guan, J.; Jakubinek, M. B.; Jakubek, Z. J.; Kingston, C. T.; Simard, B. Scalable Gas-Phase Purification of

- Boron Nitride Nanotubes by Selective Chlorine Etching. *Chemistry of Materials* **2020**, 32, 3911-3921 https://doi.org/10.1021/acs.chemmater.0c00144.
- (21) Arenal, R.; Stephan, O.; Cochon, J.-L.; Loiseau, A. Root-Growth Mechanism for Single-Walled Boron Nitride Nanotubes in Laser Vaporization Technique. *Journal of the American Chemical Society* **2007**, *129* (51), 16183–16189. https://doi.org/10.1021/ja076135n.
- (22) Jain, A.; Joseph, K.; Anthonysamy, S.; Gupta, G. S. Kinetics of Oxidation of Boron Powder. *Thermochimica Acta* **2011**, *514* (1–2), 67–73. https://doi.org/10.1016/j.tca.2010.12.004.
- (23) Yu, B.; Xing, W.; Guo, W.; Qiu, S.; Wang, X.; Lo, S.; Hu, Y. Thermal Exfoliation of Hexagonal Boron Nitride for Effective Enhancements on Thermal Stability, Flame Retardancy and Smoke Suppression of Epoxy Resin Nanocomposites via Sol-Gel Process. *Journal of Materials Chemistry A* **2016**, *4* (19), 7330–7340. https://doi.org/10.1039/c6ta01565d.
- (24) Kanehashi, K.; Saito, K. Structural Analysis of Boron Compounds Using 11B-3QMAS Solid State NMR. *Journal of Molecular Structure* **2002**, *602–603*, 105–113. https://doi.org/10.1016/S0022-2860(01)00772-4.
- (25) Arenal, R.; Ferrari, A. C.; Reich, S.; Wirtz, L.; Mevellec, J.-Y.; Lefrant, S.; Rubio, A.; Loiseau, A. Raman Spectroscopy of Single-Wall Boron Nitride Nanotubes. *Nano Letters* **2006**, *6* (8), 1812–1816. https://doi.org/10.1021/nl0602544.
- (26) Harrison, H.; Lamb, J. T.; Nowlin, K. S.; Guenthner, A. J.; Ghiassi, K. B.; Kelkar, A. D.; Alston, J. R. Quantification of Hexagonal Boron Nitride Impurities in Boron Nitride Nanotubes via FTIR Spectroscopy. *Nanoscale Advances* **2019**, *1* (5), 1693–1701. https://doi.org/10.1039/c8na00251g.
- (27) Wirtz, L.; Rubio, A.; Concha, R. A. de la; Loiseau, A. Ab Initiocalculations of the Lattice Dynamics of Boron Nitride Nanotubes. *Physical Review B* **2003**, *68* (4). https://doi.org/10.1103/physrevb.68.045425.
- (28) Borowiak-Palen, E.; Pichler, T.; Fuentes, G. G.; Bendjemil, B.; Liu, X.; Graff, A.; Behr, G.; Kalenczuk, R. J.; Knupfer, M.; Fink, J. Infrared Response of Multiwalled Boron Nitride Nanotubes. *Chem. Commun.* **2003**, No. 1, 82–83. https://doi.org/10.1039/b208214d.

